

Synthesis and Biological Activities of 2-Amino-1-arylidenamino Imidazoles as Orally Active Anticancer Agents

Wen-Tai Li,[†] Der-Ren Hwang,[†] Jen-Shin Song,[†] Ching-Ping Chen,[†] Jiunn-Jye Chuu,[†] Chih-Bo Hu,[†] Heng-Liang Lin,[†] Chen-Lung Huang,[‡] Chiung-Yi Huang,[‡] Huan-Yi Tseng,[‡] Chu-Chung Lin,[†] Tung-Wei Chen,^{†,‡} Chi-Hung Lin,[‡] Hsin-Sheng Wang,[†] Chien-Chang Shen,[†] Chung-Ming Chang,[†] Yu-Sheng Chao,[†] and Chiung-Tong Chen^{*,†}

[†]Division of Biotechnology and Pharmaceutical Research, National Health Research Institutes, 35 Keyan Road, Zhunan, Miaoli 35053, Taiwan, ROC, and [‡]Institute of Biophotonics, National Yang Ming University, Shih-Pai, Taipei 11221, Taiwan, ROC

Received October 9, 2009

2-Amino-1-arylidenaminoimidazoles, a novel class of orally (po) active microtubule-destabilizing anticancer agents, were synthesized. The compounds were designed from a hit compound identified in a drug discovery platform by using cancer cell-based high throughput screening assay. Selective synthesized compounds exerted cell cytotoxicity against human cancer cells. The underlying mechanisms for the anticancer activity were demonstrated as interacting with the tubulins and inhibiting microtubule assembly, leading to proliferation inhibition and apoptosis induction in the human tumor cells. Furthermore, two compounds showed in vivo anticancer activities in both po and intravenously (iv) administered routes and prolonged the life spans of murine leukemic P388 cells-inoculated mice. These new po active antimetabolic anticancer agents are to be further examined in preclinical studies and developed for clinical uses.

Introduction

The high-throughput screening (HTS^a) platform has been utilized in the discovery of drugs for many years.^{1–3} To identify active compounds (i.e., hits) by using HTS against a library of a large amount of compounds using cell-based colorimetric assays is a now one of the routine activities in drug discovery.^{4–7} There are currently marketed drugs and drug candidates in the developmental stages that were successfully discovered by using the HTS platform.⁷ We had identified several potential HTS hit compounds by using a colorimetric human cancer cell-based cytotoxicity HTS assay against in-house synthesized and commercially available compounds. 2-((1*E*)-(1-(1-Phenylethylideneamino)-4-phenyl-1*H*-imidazol-2-ylimino)methyl)-4,6-dibromophenol is one of the identified hit compounds and contains aminoimidazole as the chemical skeleton. 4-Amino-5-imidazole derivatives have been found to possess potent anticancer activities,^{8–10} while some bis[2-chloroethyl]aminoimidazole derivatives were DNA binding agents and topoisomerase II inhibitors.¹¹ Naamidine A, a 2-aminoimidazole alkaloid,^{12,13} was a potent antagonist of the epidermal growth factor receptor whose downstream signaling pathways, when overexpressed, leads to cancer cell growth and tumorigenesis. We designed and synthesized 2-amino-1-arylidenaminoimidazoles and found

that they were biologically active inhibiting the polymerization of tubulins.

Microtubule has been a proven molecular target via which anticancer drugs have been demonstrated with efficacies and currently used in patients.^{14–16} There are clinically used antimetabolic microtubule-destabilizers, vinca alkaloids vincristine, vinblastine, and a third-generation vinca alkaloid vinorelbine.¹⁷ Inhibiting tubulin polymerization or interfering with microtubule disassembly disrupts several cellular functions, including cell motility and mitosis. The colchicine-site binders that inhibit microtubule polymerization are another class of promising compounds in discovery and development, including combretastatin A-4 phosphate.^{18–20} New tubulin targeting agents are currently in preclinical and clinical development, among which very few are po active.²⁰

Here we described the syntheses and biological functions of novel po active anticancer agents, 2-amino-1-arylidenaminoimidazoles designed by modifying the core structure of a high-throughput screening hit identified by a human cancer cell-based cytotoxicity assay.

Chemistry

The general method for the synthesis of 2-amino-1-arylidenaminoimidazoles is shown in Scheme 1. Starting with aminoguanidine, the free amine was obtained by adding hydrochloride to liberate carbon dioxide, coupled with 4-chlorobenzaldehyde to generate guanylhydrazone (**1**) in a good yield of 91%. Ring closure reaction was accomplished by the treatment of 2-bromoacetophenone with **1** to afford 1-(4-chlorobenzylideneamino)-4-phenyl-1*H*-imidazol-2-amine (**2**) in a yield of 77%.^{21–24} The synthetic procedures illustrated in Scheme 1 were then carried out to give the desired 2-amino-1-arylidenaminoimidazoles (**2–23**) listed in Chart 1.

*To whom correspondence should be addressed. Phone: 886-37-246-166, extension 35711. Fax: 886-37-586-456. E-mail: ctchen@nhri.org.tw.

^aAbbreviations: HTS, high-throughput screening; NOE, nuclear Overhauser effect; MTS, 3-(4,5-dimethylthiazol-2-yl)-5-(3-carboxymethoxyphenyl)-2-(4-sulfophenyl)-2*H*-tetrazolium; PMS, phenazine methosulfate; DMSO, dimethyl sulfoxide; FITC, fluorescein isothiocyanate; BrdU, 5-bromo-2-deoxyuridine; LI, 5-bromo-2-deoxyuridine labeling index; OD, optical density.

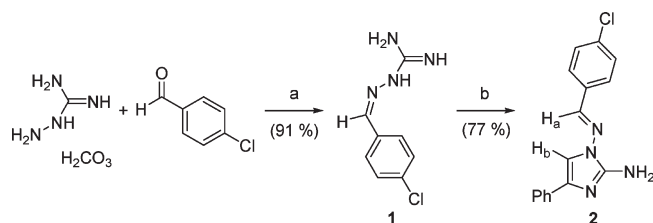
The stereochemistry of the 2-amino-1-arylidenoimidazoles were characterized by nuclear overhauser effect (NOE) experiments. (*E*)-Configuration of the exocyclic C=N bond of the 2-amino-1-arylidenoimidazoles was the only one isomer found. There was a strong NOE effect between the two protons of the exocyclic CH=N and imidazole CHb of **2**, and this result was also consistent with the previous report.²⁵ The chemical stability of the 2-amino-1-arylidenoimidazoles was also examined by the treatment of **2** in hydrochloride (pH 2) solution (CH₃CN/H₂O = 1:1) with shaking for 12 h. Although Schiff base hydrolysis happens under acidic conditions, the stability test indicated that there were no imine hydrolysis products found. The chemical stability indicated that **2** may also be stable in the acidic environment in the stomach when po administered.

The chemical structures of these 2-amino-1-arylidenoimidazoles are novel for targeting tubulins. Previously reported tubulin-targeting compounds contain a core structure with an imidazole^{26,27} or benzimidazole²⁶ different from the presently reported one. The core structures of these imidazole-containing compounds reported in the present study are different from those of the literature-reported tubulin-interacting compounds that contain an imidazole.

Biology

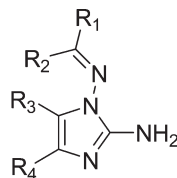
All the synthesized 2-amino-1-arylidenoimidazoles (**2–23**) were initially evaluated for cytotoxicity in the human gastric cancer NUGC-3 cells using a colorimetric 3-(4,5-dimethylthiazol-2-yl)-5-(3-carboxymethoxyphenyl)-2-(4-sulfo-phenyl)-2*H*-tetrazolium (MTS) and phenazine methosulfate (PMS) assay system^{28,29} by measuring the residual cancer cell activity after treatment with the test compounds. Selective

Scheme 1^a



^a Reagents and conditions: (a) 4-chlorobenzaldehyde, reflux, 10 min; (b) 2-bromoacetophenone, NaOH, EtOH, 70 °C, 4 h.

Chart 1. Selective 2-Amino-1-arylidenoimidazoles



- 2:** R₁ = 4-chlorophenyl, R₂ = H, R₃ = H, R₄ = phenyl
3: R₁ = 4-fluorophenyl, R₂ = H, R₃ = H, R₄ = phenyl
4: R₁ = 4-bromophenyl, R₂ = H, R₃ = H, R₄ = phenyl
5: R₁ = 4-chlorophenyl, R₂ = H, R₃ = H, R₄ = 3-pyridinyl
6: R₁ = phenyl, R₂ = H, R₃ = H, R₄ = phenyl
7: R₁ = 3-methyl-2-thienyl, R₂ = H, R₃ = H, R₄ = phenyl
8: R₁ = 4-(trifluoromethyl)phenyl, R₂ = H, R₃ = H, R₄ = phenyl
9: R₁ = 4-chloro-2-nitrophenyl, R₂ = H, R₃ = H, R₄ = phenyl
10: R₁ = 3,4-dichlorophenyl, R₂ = H, R₃ = H, R₄ = phenyl
11: R₁ = 2,3-dichlorophenyl, R₂ = H, R₃ = H, R₄ = phenyl
12: R₁ = 2-chlorophenyl, R₂ = H, R₃ = H, R₄ = phenyl

active 2-amino-1-arylidenoimidazoles were then further examined for possible molecular and cellular mechanisms of anticancer activities. Interactions with tubulins affected the microtubule assembly kinetics, induction of apoptosis as visualized by DNA fragmentation analysis in the human gastric cancer NUGC-3 cells, and inhibition of the proliferation of human tumors in the ex vivo histoculture system.²⁹ Furthermore, the in vivo antitumor activities were also explored by using the murine leukemic P388 cells-inoculated mouse model.³⁰ Compounds **2**, **3**, and **5** showed in vitro anticancer activities and were further evaluated for biological activities in the biological functional studies.

Results and Discussion

In Vitro Anticancer Activity against Human Gastric Cancer Cells. The IC₅₀ concentrations of **2–23** against human gastric cancer NUGC-3 cells were determined and summarized in Table 1. Structure–activity relationships between the substitutions of 2-amino-1-arylidenoimidazole have been evaluated. Compounds **6**, **7**, and **13** with the arylidene substituents of phenyl, 3-methyl-2-thiophenyl, and 4-quinolyl, respectively, exhibited cytotoxic IC₅₀ values of 0.84, 0.91, and > 10 μM against NUGC-3 cancer cells. Among them, phenyl substitution was superior to the others. In addition, the substituent on the phenyl ring of arylidene indicated that 4-fluorophenyl (**3**) has comparable activity to 4-chlorophenyl (**2**) with IC₅₀ values of 0.05 and 0.06 μM, respectively, whereas a 4-bromophenyl (**4**) led to a decrease in the activity. Compound **12**, with 2-chlorophenyl of arylidene, resulted in the apparent decrease of cytotoxicity compared to the 4-chlorophenyl (**2**). Therefore, substitution at the 4-position of

Table 1. Anticancer Activity of 2-Amino-1-arylidenoimidazoles against Human Gastric Cancer NUGC-3 Cells^a

compd	IC ₅₀	compd	IC ₅₀	compd	IC ₅₀
2	0.06	10	0.74	18	0.31
3	0.05	11	5.12	19	0.06
4	0.58	12	3.97	20	0.86
5	0.23	13	> 10	21	0.08
6	0.84	14	> 10	22	> 10
7	0.91	15	5.20	23	0.51
8	5.77	16	3.28	colchicine	0.01
9	> 10	17	0.05		

^a IC₅₀ values expressed in μM as the mean values of triplicate wells from at least three experiments.

- 13:** R₁ = 4-quinolyl, R₂ = H, R₃ = H, R₄ = phenyl
14: R₁ = 4-chlorophenyl, R₂ = H, R₃ = H, R₄ = biphenyl
15: R₁ = 4-chlorophenyl, R₂ = H, R₃ = H, R₄ = 2-methoxyphenyl
16: R₁ = 4-chlorophenyl, R₂ = H, R₃ = H, R₄ = 5-chloro-2-thienyl
17: R₁ = 4-chlorophenyl, R₂ = H, R₃ = H, R₄ = 3-thiophenyl
18: R₁ = 4-chlorophenyl, R₂ = H, R₃ = H, R₄ = 2-pyridinyl
19: R₁ = 4-fluorophenyl, R₂ = H, R₃ = H, R₄ = 3-pyridinyl
20: R₁, R₂ = 1,2,3,4-tetrahydro-1-naphthalenyl, R₃ = H, R₄ = phenyl
21: R₁ = 4-chlorophenyl, R₂ = H, R₃ = H, R₄ = 2-thiophenyl
22: R₁ = 4-chlorophenyl, R₂ = H, R₃ = phenyl, R₄ = phenyl
23: R₁ = 4-chlorophenyl, R₂ = H, R₃ = H, R₄ = 1,3-thiazol-2-yl

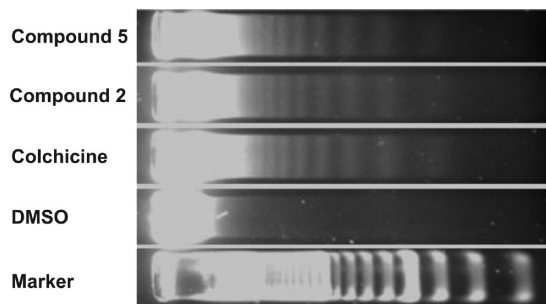


Figure 1. Apoptotic DNA fragmentation induction was observed in human gastric NUGC-3 cancer cells treated with **2**, **5**, and colchicine at 100 nM for 24 h.

the phenyl ring seems to play a critical role for the cytotoxic activity. A similar phenomenon was also observed with substituents of 3,4-dichlorophenyl (**10**) and 2,3-dichlorophenyl (**11**) on arylidene and showed IC_{50} values of 0.74 and 5.12 μ M, respectively. Interestingly, 4-chloro-2-nitrophenyl of arylidene (**9**) showed no activity against the NUGC-3 cancer cells. The structure–activity relationship with the comparisons of **17** and **21** versus **18** and **23** revealed that 2-thiophenyl and 3-thiophenyl at the 4-position of the imidazole ring exhibited the most potent cytotoxic activities against the NUGC-3 cancer cells. Compound **5**, with a 3-pyridyl group at the 4-position of imidazole, revealed a similar activity to **18** containing a 2-pyridyl group. In addition, **19**, with substitution of 4-fluorophenyl of arylidene and 3-pyridyl group at the 4-position of imidazole, exhibited a potent cytotoxic IC_{50} of 0.06 μ M. Substitution on the 5-position of imidazole caused loss of activity, similar to that shown by compound **22**.

DNA Fragmentation Induction in Human Gastric Cancer Cells. Human gastric NUGC-3 cancer cells were treated with 2-amino-1-arylideneaminoimidazoles for 24 h, and the induction of apoptosis was demonstrated by DNA fragmentation analysis. As shown in Figure 1, compounds **2** and **5** at 100 nM induced DNA fragmentation in the cancer cells. Apoptosis induction may be a mechanism by which these 2-amino-1-arylideneaminoimidazoles killed the cancer cells. A dimethyl sulfoxide (DMSO) vehicle negative control and colchicine as positive control were included.

Inhibition of Tubulin Polymerization. Tubulin polymerization assays were performed to explore whether microtubule is the potential target through which the 2-amino-1-arylideneaminoimidazoles exerted anticancer activities. With the inclusion of the reference colchicine, **2** and **5** interacted with and inhibited the microtubule assembly, as shown in Figure 2. The estimated IC_{50} values are summarized in Table 2. As previously reported for antimicrotubule agents,^{31,32} the potencies for inhibiting the microtubule assembly were not necessarily correlated to those for inhibiting the cancer cell proliferation. The inhibition on the tubulin polymerization and colchicine binding kinetics provide evidence at the molecular level for the interference on microtubule assembly, which is one of the proven molecular mechanisms of anticancer action and for the compounds presented in the study. Furthermore, the calculated partition coefficients (calculated $\log P$) of compounds **2** and **5** are 4.152 and 2.655, respectively. The difference in the hydrophobic characteristics is likely to be attributed, in part, to the different potencies between the molecular and cellular systems.

Inhibition of Colchicine Binding to Tubulins. Both compounds **2** and **5** concentration-dependently interfered with

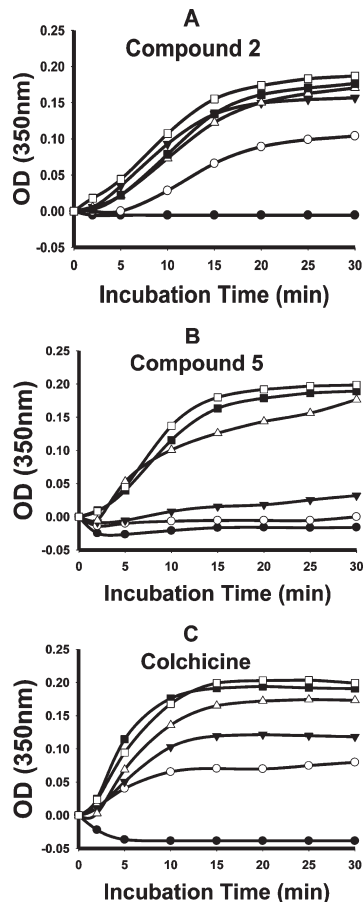


Figure 2. Inhibition on tubulin polymerization by **2** (A), **5**, (B), and colchicine (C) at the following concentrations (μ M): (●) 10, (○) 1, (▼) 0.1, (△) 0.01, (■) 0.001, (□) vehicle control.

Table 2. Inhibition of Tubulin Polymerization by **2**, **5**, and Colchicine

compd	IC_{50} (μ M) ^a
2	2.65 ± 0.41
5	0.27 ± 0.03
colchicine	0.29 ± 0.05

^a IC_{50} expressed as the mean ± SD.

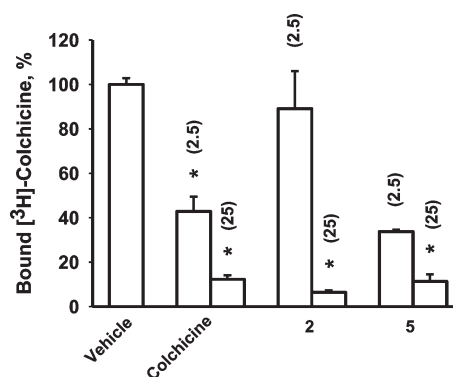


Figure 3. [³H]Colchicine binding to tubulins was concentration-dependently inhibited by treatments of **2** and **5**.

[³H]colchicine binding to tubulins as illustrated in Figure 3. Compounds **2** and **5** at 25 μ M potently interfered with the colchicine binding to tubulins and showed activity comparable to that caused by cold colchicine of the same concentration. A concentration-dependent inhibition on the colchicine

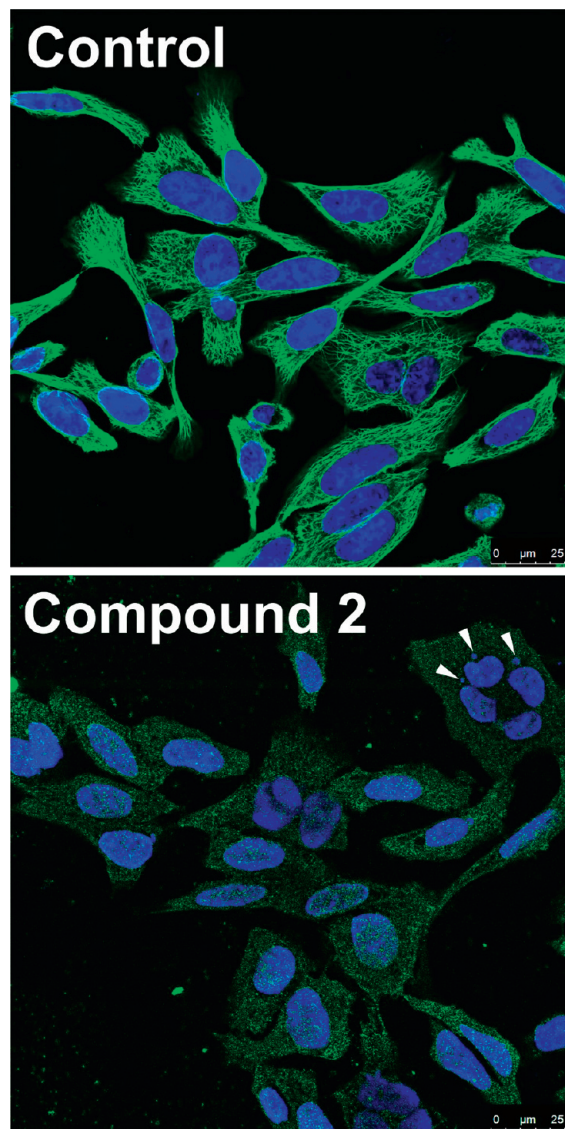


Figure 4. Aberration of microtubule arrangements in the human gastric cancer NUGC-3 cells treated by **2** at $1 \mu\text{M}$ for 16 h. DNA was stained by Hoechst 33258 (blue), and tubulins were visualized by FITC (green). Disorganized green fluorescent microtubule structures and slightly fragmented nucleus DNAs indicated by arrowheads in the **2**-treated cancer cells were observed.

binding kinetics was observed and thus demonstrated the specificity of interactions on the colchicine binding sites and the quality of the assay system.

Interference on the Microtubule Assembly in Human Gastric Cancer Cells. Treated by **2** at $1 \mu\text{M}$ for 16 h, NUGC-3 gastric cancer cells were immunostained for microtubules as visualized by fluorescein isothiocyanate (FITC), in green shown in Figure 4. A DMSO vehicle control was included. Compared to the well-arranged microtubule structures in the untreated cancer cells, the disarranged microtubule structures were observed as diffused green fluorescent tubulin-immunoreactive activities in those **2**-treated NUGC-3 cells. It was also noted that the blue fluorescence-stained DNA of the treated cancer cells were fragmented, as also observed in Figure 1 from the DNA fragmentation assay. The cells then underwent apoptotic processes and eventually died, as shown in the cytotoxicity assay. Therefore, the molecular interaction effects of 2-amino-1-arylidenoimidazoles

on the targeted microtubules were not only demonstrated by the inhibitions on the tubulin polymerization and colchicine binding but also visualized by fluorescence imaging observations of the microtubules.

Ex Vivo Antitumor Activity against Human Tumors. Histocultured human gastric MKN-45 and colorectal SW-480 tumors were treated with **2** and **3** for 96 h. The representative tumor tissue sections immunostained with DNA-incorporated 5-bromo-2-deoxyuridine (BrdU) brown and hematoxylin-counterstained blue nuclei of the tumor cells are shown in Figure 5. As in Figure 5A–D, **2** caused a concentration-dependent reduction in the number of the BrdU-labeled human gastric MKN-45 tumor cells. A similar phenomenon was also observed in the human colorectal SW-480 tumors treated with **2** as shown in Figure 5E–G. Compound **3** also demonstrated antiproliferative activities against both gastric and colorectal tumors because a small number of residual BrdU-labeled tumor cells were observed at the highest concentration ($10 \mu\text{g/mL}$) treated. It was, however, noted in Figure 5H that the nuclei of the residual BrdU-labeled gastric tumor cells after **3** treatments were mainly fragmented or presented in debris, indicating that the cells were undergoing apoptosis. The BrdU labeling index (LI) of each treated tumor specimens was counted and the calculated data for the treatments with **2** and **3** in the human gastric MKN-45 tumors were plotted in Figure 6A and Figure 6B, respectively. The IC_{50} concentrations that reduced 50% of the LI (i.e., the tumor cell proliferation activity) in the histocultured human gastric tumors for **2** and **3** were 13 and $34 \mu\text{M}$, respectively.

In Vivo Activity on Prolongation of Leukemic Mouse Cancer Survival. Female DBA/2J mice of a vehicle control group consistently survived for 6–7 days after single iv inoculation of the murine leukemic P388 cancer cells. A positive quality control group using doxorubicin (10 mg/kg , once, iv) was also included in each experiment to demonstrate a consistent effect (approximately 110% increase in life span) of doxorubicin in prolonging the survival period in the leukemic DBA/2J mice and thus the proper response sensitivity of the testing system. Compound **2** exhibited both po and iv dose-dependent activities in increasing the life spans of the cancer cells-bearing animals as shown in Figure 7A without evident loss of body weight (data not shown). A significant dose-dependent relationship ($p < 0.05$, ANOVA) was observed. The oral doses of **2** at 25, 100, and 200 (mg/kg)/day for 9 consecutive days increased the life spans by 14%, 71%, and 114%, respectively. On the other hand, iv doses of **2** at 2.5 and 7.5 (mg/kg)/day for 4 consecutive days increased the life spans by 17% and 100%, respectively. Compound **3** ($200 \text{ (mg/kg)/day} \times 9 \text{ days}$, po) exhibited a 110% prolongation of the survival of leukemic animals as shown in Figure 7B.

Conclusions

Cancer has been the leading cause of death worldwide. Chemotherapy remains one of the major treatment options available for cancer, and most of the currently used anticancer drugs are administered to patients via a parenteral infusion or bolus injection. Clinical complications with the parenteral administrations have been documented. Extra care is needed because of inappropriate patient compliances, and extra cost associated with hospitalization is necessary. Efforts in searching for po active anticancer agents have been extensive,

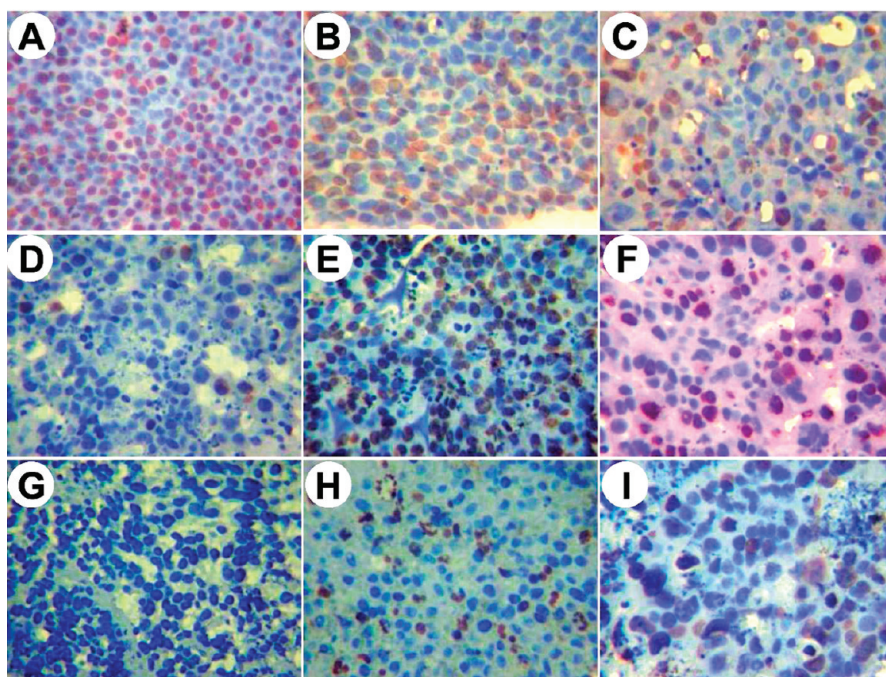


Figure 5. Inhibition activities of **2** and **3** against on the tumor cell proliferation in ex vivo histocultured human gastric MKN-45 and colorectal SW-480 tumors. Representative tumor tissue sections with immunostained DNA-incorporated BrdU (in brown nuclei and/or fragmented apoptotic bodies) and hematoxylin-counterstained (in blue nuclei) tumor cells were shown as in MKN-45 tumors treated with vehicle (A) and with **2** at 0.01 (B), 1 (C), and 10 (D) $\mu\text{g}/\text{mL}$; in SW-480 tumors treated with vehicle (E) and with **2** at 1 (F) and 10 (G) $\mu\text{g}/\text{mL}$; in MKN-45 tumors with **3** at 10 $\mu\text{g}/\text{mL}$ (H); and in SW-480 tumors treated with **3** at 10 $\mu\text{g}/\text{mL}$ (I).

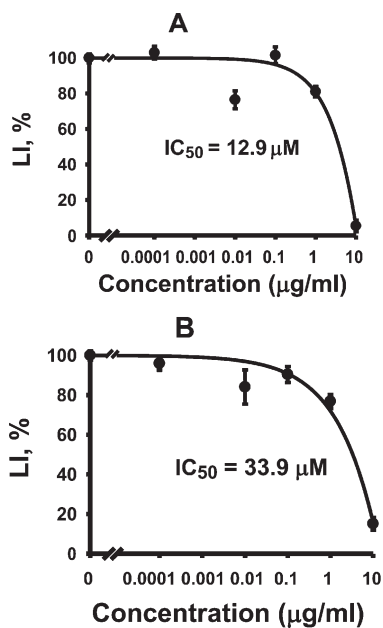


Figure 6. Concentration-dependent anticancer activities of **2** and **3** against ex vivo histocultured human gastric MKN-45 tumors. The labeling indices (LIs) were calculated from the histocultured gastric MKN-45 tumors treated with **2** (A) and **3** (B) for 96 h, and the IC_{50} values were estimated as indicated.

including the anticancer drug category of tubulin binding agents from which only injectable drugs are available such as taxanes and vinca alkaloids. We report here the synthesis and biological functions of 2-amino-1-arylideneaminoimidazoles as po active anticancer agents. Selective compounds had shown potent effects in the interference on the colchicine binding to tubulins, inhibition of tumor cell proliferation,

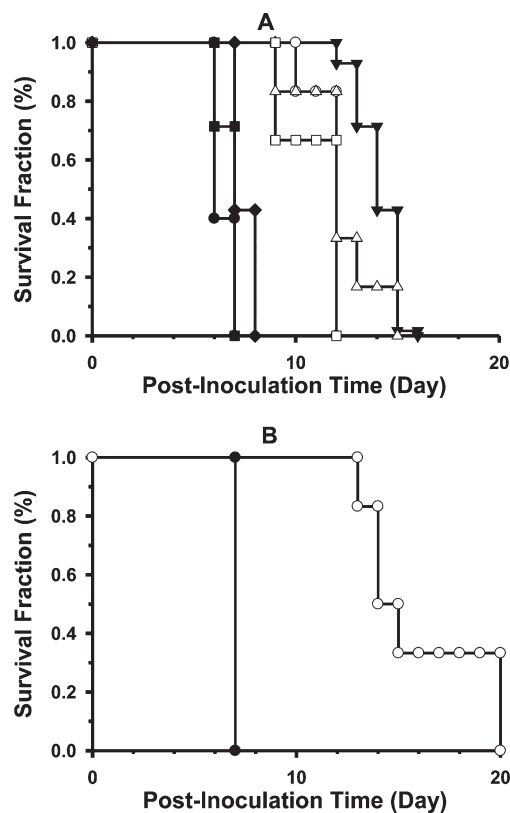


Figure 7. Dose-dependent prolongation in the survival of P388 cells-inoculated leukemia DBA/2J mice po gavaged or iv administered with **2** (A) and **3** (B). (A) (\blacktriangledown) 200 (po \times 9), (\circ) 200 (po \times 4), (\triangle) 100 (po \times 9), (\blacksquare) 25 (po \times 9), (\square) 7.5 (iv \times 4), (\blacklozenge) 2.5 (iv \times 4) mg/kg, (\bullet) vehicle control. A significant oral dose-dependent relationship ($p < 0.05$, ANOVA) was observed. (B) (\circ) 200 mg/kg (po \times 4), (\bullet) vehicle control.

and induction of human cancer cell apoptosis. Given *po* or *iv*, the compounds demonstrated *in vivo* anticancer activities and prolonged the survival of leukemia mice. The 2-amino-1-arylideneaminoimidazoles may therefore be further developed as anticancer therapeutics in patients.

Experimental Section

In Vitro Growth Inhibition Study. As previously reported,³⁰ human gastric cancer NUGC-3 cells were seeded at a density of 4500 cells in 100 μ L per well in 96-well flat-bottom plates and incubated for 24 h at 37 °C in a 5% CO₂ incubator. Test compounds were dissolved in DMSO purchased from Sigma (St. Louis, MO), further diluted with the culture media to obtain an optimal range of concentrations for treatments in duplicate per concentration (200 μ L/well), and incubated at 37 °C in a CO₂ incubator for 72 h. All treatment media contained the final DMSO concentration of \leq 0.3%. Actinomycin D of 10 nM and 0.3% DMSO were used as the positive and vehicle controls, respectively. A colorimetric assay using the MTS/PMS system was used to determine the cytotoxic activity of the test compounds. Both MTS and PMS were purchased from Promega Corp. (Madison, WI). The optical density (OD) values at 490 nm were measured with a 1420-multilabel counter VICTOR from Wallac (Turku, Finland). The IC₅₀, the concentration that inhibited 50% of the cancer cell growth activity, was then determined.

DNA Fragmentation Analysis. Oligonucleosomal fragments of the genomic DNA induced by treatments with the compounds in human gastric cancer NUGC-3 cells were isolated and analyzed by agarose gel electrophoresis according to previously described procedures³⁰ with modification. In brief, 2×10^6 cancer cells were incubated with the test compound for 24 h. Both floating and adherent cells were collected at the end of incubation, washed once with PBS, and resuspended in the lysis buffer. After incubation at 50 °C overnight, the samples were treated with RNase A at 37 °C for 1 h. The DNA was extracted with phenol/chloroform/isoamyl alcohol (25:24:1), and the supernatant was collected, separated on a 2% agarose gel, and stained with ethidium bromide. Colchicine was used as a positive control.

Tubulin Polymerization Assay. Microtubule turbidity assay was conducted according to a previously reported procedure with modifications.³³ In brief, bovine brain microtubule-associated protein-rich heterodimeric tubulins from Cytoskeleton Inc. (Denver, CO) were dissolved in a 100 μ L of polymerization buffer containing 100 mM PIPES (pH 6.9), 2 mM MgCl₂, 1 mM GTP, and 2% (v/v) DMSO and placed in 96-well microtiter plates in the presence of **2** or **5**. The increase in absorbance at 340 nm was measured in a microplate reader PowerWave X from Bio-Tek Instruments (Winooski, VT) at 37 °C and recorded at optimal time points for 30 min. The area under the curve normalized to that of vehicle control was used to estimate an IC₅₀ that inhibited tubulin polymerization by 50% using nonlinear regression with SigmaPlot from SPSS Inc. (Chicago, IL). Colchicine was served as a reference control.

Colchicine Binding Assay. Binding of [³H]colchicine (ring C, methoxy-3H]colchicine, from PerkinElmer, Waltham, MA) to bovine brain microtubule associated protein-rich tubulins (Cytoskeleton Inc., Denver, CO) was measured by column centrifugation as previously described with modifications.^{33,34} Solution mixtures of the heterodimeric tubulins and [³H]colchicine (0.1 Ci/mmol), both at 2.5 μ M in the presence of the compound or cold colchicine, were incubated in the polymerization buffer at room temperature for 1 h. An amount of 50 μ L of the solutions was centrifuged through a Sephadex G-50 column, and the eluates were analyzed for radioactivity in counts per min (cpm) by scintillation counting. The percentage of the compound bound was calculated using the equation [(cpm with compound) - (cpm without tubulin)]/[(cpm with DMSO) - (cpm without tubulin)] \times 100.

Visualizations of DNA and Tubulins in Cancer Cells. Human gastric cancer NUGC-3 cells were treated with 1 μ M test compound for 16 h. The cells were washed with phosphate-buffered solution (PBS) and fixed with 4% formaldehyde at room temperature for 10 min. After being rinsed with PBS, the fixed cells were then blocked with 5 mg/mL bovine serum albumin at room temperature for 30 min followed by an incubation with 1:200 dilution of monoclonal anti- β -tubulin (mouse IgG1 isotype, catalog no. T42026, Sigma, St. Louis, MO) at 4 °C overnight. The antitubulin IgG1-recognized tubulins were then visualized as green fluorescence by a reaction with 1:300 dilution of the goat anti-mouse IgG FITC (catalog no. F0257, Sigma) at room temperature for 1 h. The cells were then incubated for DNA staining in the Hoechst 33258 (1 μ g/mL) in 0.1% Triton X-100 PBS at room temperature for 5 min. The cellular images were visualized and photos taken by using a fluorescence confocal laser-scanning microscope (Leica TCS SP2, Heidelberg, Germany).

Ex Vivo Histocultures of Xenografted Human Tumors. As reported previously,²⁹ histocultures of human gastric MKN-45 and colorectal SW480 tumors were established. The tumor cells of 1×10^6 were inoculated subcutaneously to the nude mice and monitored for tumor growth twice weekly. The subcutaneously growing tumor xenografts at a size of approximately 1 cm³ in nude mice were then harvested and dissected into pieces of 1–2 mm in diameter. Gelatin gels cut into pieces of 1 cm³ were presoaked overnight in culture medium in six-well culture plates. Five to six of the tumor pieces were placed on each gelatin gel and cultured in medium consisting of MEM/DMEM (1:1), 2 mM L-glutamine, 10% FBS, 1 mM sodium pyruvate, 0.1 mM nonessential amino acids, and 40 μ g/mL gentamicin (pH 7.4) at 7 mL per well. The histocultures were kept in a humidified atmosphere containing 95% air and 5% CO₂ at 37 °C in a CO₂ incubator from Binder GmbH (Tuttlingen, Germany). After a 3-day incubation, the histoculture media were replaced with freshly prepared culture media containing the test compound at various concentrations ranging from 0.0001 to 10 μ g/mL. The histocultures were further incubated for 96 h in a CO₂ incubator. After the compound treatments, the histocultures were incubated with 40 μ M BrdU for 48 h, washed 3 times with PBS, fixed in 10% neutralized formalin, dehydrated in ethanol solutions, and then embedded in paraffin for tissue sectioning. Tumor tissue sections of 5 cm thickness were prepared and immunostained with BrdU antibody (M744) for the DNA-incorporated BrdU in the proliferating tumor cells. Proliferating tumor cells were visualized in brown nuclei, whereas nonproliferating cells were counterstained in blue nuclei with Mayer's hematoxylin from Shandon (Pittsburgh, PA). LI was defined as the number of the BrdU-labeled (brown) tumor cells divided by the number of total (brown and blue) tumor cells and used as an index for the proliferation ability of the histocultured tumor cells.

In Vivo Cancer Survival Study. The *in vivo* anticancer activities of the compounds were evaluated by a murine leukemic mouse model.³⁰ Inbred female DBA/2J mice of 5 weeks old were purchased from The National Laboratory Animals Center (Taipei, Taiwan). Murine leukemic P388 cells purchased from the Japanese Collection of Research Bioresources (Osaka, Japan) were cultured and propagated in RPMI 1640 medium supplemented with the MEM-nonessential amino acids, 50 μ M 2-mercaptoethanol, and 10% fetal bovine serum. All mice were *iv* inoculated with 1×10^6 P388 cells per mouse. The treatments were initiated in one day after the cell inoculation. Seven to eight mice per treatment group were used in the treated and vehicle control groups. Test compounds were dissolved in DMSO and then diluted with the dosing vehicle 0.5% carboxymethyl cellulose with a final concentration of DMSO of less than 0.5%. The compounds were *po* gavaged to the mice (0.1 mL per mouse). Mice of the negative control group were treated with the dosing vehicle only. The P388 cell-inoculated leukemic animals were monitored twice daily for survival, and the survival fractions of the treatment groups were recorded. The time period for which

50% of the leukemic mice survived was defined as the median survival time and used to calculate the percentage (normalized to the median survival time of the control group) of increase in the life span of the treated animals. The percentage of increase in life span was then used as an index for treatment response.

Chemistry. All commercially available materials were used without further purification unless otherwise stated. For anhydrous reactions, glassware was dried overnight in an oven at 120 °C and cooled in a desiccator over anhydrous CaSO₄ or silica gel. Diethyl ether and tetrahydrofuran were obtained by distillation from the sodium ketyl of benzophenone under nitrogen. Other solvents, including chloroform, dichloromethane, ethyl acetate, and methanol, were distilled over CaH₂ under nitrogen. Melting points were obtained with a Yanaco (MP-500D) melting point apparatus. Infrared spectra were recorded on a Perkin-Elmer (Spectrum RX1) spectrophotometer. The proton NMR spectra were obtained on a Varian Mer-Vx-300 (300 MHz) spectrometer. Chloroform-*d* and DMSO-*d*₆ of spectrograde were used as solvents. All NMR chemical shifts are reported as δ values in parts per million (ppm), and coupling constants (*J*) are given in hertz (Hz). The splitting pattern abbreviations are as follows: s, singlet; d, doublet; t, triplet; q, quartet; br, broad; m, unresolved multiplet due to the field strength of the instrument; dd, doublet of doublet; dt, doublet of triplet; ddd, doublet of doublet of doublet. Mass spectra were carried out on a Hewlett-Packard (model 1100 MSD) mass spectrometer.

Purification was performed by using preparative separations in gravity column chromatography (Merck silica gel 60, particle size of 230–400 mesh). Analytical TLC was carried out on precoated plates (Merck silica gel 60, F₂₅₄). Compounds analyzed on the TLC plates were visualized by using UV light, I₂ vapor, or 2.5% phosphomolybdic acid in ethanol with heating. The purity of the synthetic compounds was checked by HPLC with the detection wavelength of 254 nm. The purity of individual compounds was determined from the area peaks in the chromatogram of the sample solution. UV spectra (λ , nm) were determined on an Agilent 1024-element diode array. All the presented compounds showed a purity of >95%.

General Procedure for the Synthesis of 2–23. **1-(4-Chlorobenzylideneamino)-4-phenyl-1H-imidazol-2-amine (2).** Hydrochloric acid (20%, 4 mL) and 4-chlorobenzaldehyde (2.0 g, 15.8 mmol) were mixed together, and this mixture was slowly added to a solution of aminoguanidine bicarbonate (2.2 g, 15.8 mmol) in water (12 mL). After liberation of carbon dioxide, the mixture was heated to reflux and then allowed to cool to room temperature. A solution of 40% aqueous potassium hydroxide (7 mL) was added, and the mixture was heated at reflux for an additional 10 min. The resulting solution was filtered, washed with water until the wash water was at pH 7, dried, and recrystallized from ethanol to give (4-chlorobenzylideneamino)guanidine **1** (2.6 g, 91%) as a yellow solid.

Compound **1** (0.74 g, 4.06 mmol) was added to a solution of 2-bromoacetophenone (0.40 g, 2.03 mmol) in ethanol (10 mL), and the mixture was heated to 70 °C for 4 h. Aqueous sodium hydroxide solution was added dropwise. A yellow precipitate was formed in the reaction mixture which was cooled to room temperature for an additional 10 h. The precipitates were then filtered, washed with hot water, and recrystallized from ethanol to give **2** (0.44 g, 77%) as a yellow solid. ¹H NMR (CDCl₃): δ 8.56 (s, 1H), 8.01–7.96 (m, 3H), 7.69 (d, *J* = 7.2 Hz, 2H), 7.37–7.30 (m, 4H), 7.18 (t, *J* = 7.2 Hz, 1H), 6.20 (s, 2H). ¹³C NMR (CDCl₃): δ 169.2, 157.0, 140.5, 136.0, 133.1, 130.8, 129.4, 129.3, 128.8, 127.5, 122.0, 115.6. ESMS *m/z*: 281.5 (MH⁺).

1-(4-Fluorobenzylideneamino)-4-phenyl-1H-imidazol-2-amine (3). ¹H NMR (CDCl₃): δ 8.55 (s, 1H), 7.97–7.92 (m, 3H), 7.69 (d, *J* = 6.0 Hz, 2H), 7.57 (d, *J* = 7.8 Hz, 2H), 7.34 (t, *J* = 6.0 Hz, 2H), 7.19 (t, *J* = 6.0 Hz, 1H), 6.25 (s, 2H). ¹³C NMR (CDCl₃): δ 161.0, 142.5, 138.6, 137.0, 133.1, 131.9, 131.6, 129.3, 129.0, 127.8, 126.7, 125.5, 122.0. ESMS *m/z*: 297.5 (M + 1)⁺.

1-(4-Bromobenzylideneamino)-4-phenyl-1H-imidazol-2-amine (4). ¹H NMR (CDCl₃): δ 8.53 (s, 1H), 7.96 (s, 1H), 7.84 (d, *J* = 8.4 Hz, 2H), 7.69 (d, *J* = 8.4 Hz, 4H), 7.34 (t, *J* = 7.5 Hz, 2H), 7.19 (t, *J* = 7.2 Hz, 1H), 6.25 (br, 2H). ¹³C NMR (CDCl₃): δ 157.0, 140.5, 135.4, 133.9, 132.8, 131.8, 130.4, 129.3, 128.8, 127.5, 125.4, 119.0. ESMS *m/z*: 341.5 (M + 1)⁺.

1-(4-Chlorobenzylideneamino)-4-(pyridin-3-yl)-1H-imidazol-2-amine (5). ¹H NMR (CDCl₃): δ 8.89 (s, 1H), 8.55 (s, 1H), 8.38 (d, *J* = 5.1 Hz, 1H), 8.10 (s, 1H), 7.99–7.93 (m, 3H), 7.57 (d, *J* = 7.5 Hz, 2H), 7.37 (t, *J* = 5.1 Hz, 1H), 6.34 (br, 2H). ¹³C NMR (CDCl₃): δ 162.0, 155.1, 151.0, 148.5, 137.6, 135.0, 132.1, 131.1, 130.9, 129.6, 126.0, 122.0, 117.0. ESMS *m/z*: 298.5 (M + 1)⁺.

1-(Benzylideneamino)-4-phenyl-1H-imidazol-2-amine (6). ¹H NMR (CDCl₃): δ 8.56 (s, 1H), 8.00 (s, 1H), 7.94–7.90 (m, 3H), 7.70 (d, *J* = 7.2 Hz, 2H), 7.52–7.47 (m, 3H), 7.34 (t, *J* = 7.5 Hz, 2H), 7.18 (t, *J* = 7.2 Hz, 1H), 6.19 (s, 2H). ¹³C NMR (CDCl₃): δ 155.4, 140.5, 136.0, 134.7, 131.6, 131.1, 130.6, 129.3, 128.9, 128.8, 127.5, 118.4. ESMS *m/z*: 263.6 (M + 1)⁺.

1-((3-Methylthiophen-2-yl)methyleneamino)-4-phenyl-1H-imidazol-2-amine (7). ¹H NMR (CDCl₃): δ 8.89 (s, 1H), 8.55 (s, 1H), 8.38 (d, *J* = 5.1 Hz, 1H), 8.10 (s, 1H), 7.99–7.93 (m, 3H), 7.57 (d, *J* = 7.5 Hz, 2H), 7.37 (t, *J* = 5.1 Hz, 1H), 6.34 (br, 2H). ¹³C NMR (CDCl₃): δ 163.7, 140.5, 139.5, 136.0, 133.1, 128.7, 126.8, 126.3, 124.9, 124.5, 123.2, 121.0, 11.7. ESMS *m/z*: 283.5 (M + 1)⁺, 305.6 (M + 23)⁺.

1-(4-(Trifluoromethyl)benzylideneamino)-4-phenyl-1H-imidazol-2-amine (8). ¹H NMR (CDCl₃): δ 8.64 (s, 1H), 8.13 (d, *J* = 8.1 Hz, 2H), 8.00 (s, 1H), 7.85 (d, *J* = 8.1 Hz, 2H), 7.70 (d, *J* = 7.5 Hz, 2H), 7.35 (t, *J* = 7.5 Hz, 2H), 7.20 (t, *J* = 7.5 Hz, 1H), 6.32 (s, 2H). ¹³C NMR (CDCl₃): δ 159.3, 138.5, 136.1, 135.2, 132.9, 131.1, 129.5, 129.3, 127.8, 125.5, 123.3, 122.2, 119.0. ESMS *m/z*: 331.5 (M + 1)⁺.

1-(4-Chloro-2-nitrobenzylideneamino)-4-phenyl-1H-imidazol-2-amine (9). ¹H NMR (CDCl₃): δ 8.76 (s, 1H), 8.48 (d, *J* = 8.4 Hz, 1H), 8.24 (d, *J* = 1.8 Hz, 1H), 8.19 (s, 1H), 7.95 (dd, *J* = 8.4, 1.8 Hz, 1H), 7.74 (d, *J* = 7.2 Hz, 2H), 7.41 (t, *J* = 7.2 Hz, 2H), 7.28 (t, *J* = 7.2 Hz, 1H), 7.16 (br, 2H). ¹³C NMR (CDCl₃): δ 160.1, 154.3, 143.5, 138.5, 134.0, 133.1, 131.1, 129.5, 126.3, 125.8, 123.5, 122.4, 121.1, 118.0. ESMS *m/z*: 342.5 (M + 1)⁺.

1-(3,4-Dichlorobenzylideneamino)-4-phenyl-1H-imidazol-2-amine (10). ¹H NMR (CDCl₃): δ 8.52 (s, 1H), 8.28 (d, *J* = 1.5 Hz, 1H), 7.91 (s, 1H), 7.82 (dd, *J* = 8.4, 1.5 Hz, 1H), 7.76 (d, *J* = 8.4 Hz, 1H), 7.69 (d, *J* = 7.5 Hz, 2H), 7.35 (t, *J* = 7.5 Hz, 2H), 7.19 (t, *J* = 7.5 Hz, 1H), 6.39 (s, 2H). ¹³C NMR (CDCl₃): δ 157.8.0, 142.5, 137.0, 136.7, 133.5, 131.3, 130.1, 129.7, 128.4, 127.8, 126.7, 124.5, 121.0, 21.3. ESMS *m/z*: 331.1 (M + 1)⁺.

1-(2,3-Dichlorobenzylideneamino)-4-phenyl-1H-imidazol-2-amine (11). ¹H NMR (CDCl₃): δ 8.95 (s, 1H), 8.70 (s, 1H), 8.47–8.42 (m, 3H), 7.85 (d, *J* = 7.8 Hz, 1H), 7.77 (d, *J* = 7.8 Hz, 2H), 7.57–7.49 (m, 3H), 7.42 (t, *J* = 7.8 Hz, 1H). ¹³C NMR (CDCl₃): δ 161.2, 142.5, 136.5, 135.8, 134.5, 131.1, 130.6, 128.9, 127.3, 126.8, 124.7, 122.4, 121.5, 118.0. ESMS *m/z*: 331.5 (M + 1)⁺.

1-(2-Chlorobenzylideneamino)-4-phenyl-1H-imidazol-2-amine (12). ¹H NMR (CDCl₃): δ 8.65 (s, 1H), 8.34 (d, *J* = 7.2 Hz, 1H), 8.16 (s, 1H), 7.76 (d, *J* = 7.8 Hz, 2H), 7.56 (d, *J* = 7.5 Hz, 1H), 7.51–7.41 (m, 2H), 7.34 (t, *J* = 7.8 Hz, 2H), 7.19 (t, *J* = 7.8 Hz, 1H), 6.31 (s, 2H). ¹³C NMR (CDCl₃): δ 154.0, 147.5, 137.6, 135.0, 134.5, 133.9, 132.3, 130.8, 129.3, 127.0, 124.8, 121.5, 119.0. ESMS *m/z*: 297.6 (M + 1)⁺, 319.5 (M + 1)⁺.

1-((Quinolin-4-yl)methyleneamino)-4-phenyl-1H-imidazol-2-amine (13). ¹H NMR (CDCl₃): δ 9.24 (s, 1H), 9.02–8.98 (m, 2H), 8.81 (d, *J* = 8.4 Hz, 1H), 8.39 (t, *J* = 3.9 Hz, 1H), 8.30 (d, *J* = 4.5 Hz, 1H), 8.19 (d, *J* = 4.5 Hz, 1H), 8.10 (dd, *J* = 8.4, 3.9 Hz, 1H), 7.74 (d, *J* = 7.5 Hz, 2H), 7.39 (t, *J* = 7.5 Hz, 2H), 7.22 (t, *J* = 7.5 Hz, 1H). ¹³C NMR (CDCl₃): δ 161.0, 153.1, 144.0, 139.5, 137.4, 134.0, 131.1, 128.9, 127.4, 127.3, 125.0, 124.8, 123.5, 122.0, 121.0, 115.0. ESMS *m/z*: 314.4 (M + 1)⁺.

1-(4-Chlorobenzylideneamino)-4-biphenyl-1H-imidazol-2-amine (14). ¹H NMR (CDCl₃): δ 8.57 (s, 1H), 8.04 (s, 1H), 7.95 (d,

$J = 8.4$ Hz, 2H), 7.78 (d, $J = 8.4$ Hz, 2H), 7.71–7.65 (m, 4H), 7.57 (d, $J = 8.4$ Hz, 2H), 7.45 (t, $J = 7.5$ Hz, 2H), 7.34 (t, $J = 7.5$ Hz, 1H), 6.29 (s, 2H). ^{13}C NMR (CDCl_3): δ 157.9, 142.5, 137.9, 137.6, 136.5, 136.1, 132.0, 131.9, 130.6, 129.3, 129.0, 128.4, 127.0, 125.9, 122.7, 118.0. ESMS m/z : 273.5 ($M + 1$) $^+$.

1-(4-Chlorobenzylideneamino)-4-(2-methoxyphenyl)-1H-imidazol-2-amine (15). ^1H NMR (CDCl_3): δ 8.60 (s, 1H), 8.01–7.98 (m, 3H), 7.86 (s, 1H), 7.56 (d, $J = 8.1$ Hz, 2H), 7.22–7.16 (m, 1H), 7.05–6.94 (m, 2H), 6.19 (s, 2H), 3.95 (s, 3H). ^{13}C NMR (CDCl_3): δ 161.2, 144.5, 137.6, 135.0, 133.9, 131.6, 127.8, 126.0, 137.5, 124.0, 122.6, 108.0, 52.2. ESMS m/z : 327.6 ($M + 1$) $^+$.

1-(4-Chlorobenzylideneamino)-4-(5-chlorothiophen-2-yl)-1H-imidazol-2-amine (16). ^1H NMR (CDCl_3): δ 8.51 (s, 1H), 7.94 (d, $J = 7.8$ Hz, 2H), 7.86 (s, 1H), 7.57 (d, $J = 7.8$ Hz, 2H), 7.05 (s, 2H), 6.39 (s, 2H). ^{13}C NMR (CDCl_3): δ 158.4, 147.8, 139.6, 137.0, 134.9, 133.6, 131.0, 128.5, 126.2, 125.1, 123.1, 119.0. ESMS m/z : 337.4 ($M + 1$) $^+$.

1-(4-Chlorobenzylideneamino)-4-(thiophen-3-yl)-1H-imidazol-2-amine (17). ^1H NMR (CDCl_3): δ 8.49 (s, 1H), 7.94 (d, $J = 8.4$ Hz, 2H), 7.79 (s, 1H), 7.58–7.51 (m, 4H), 7.32 (d, $J = 4.8$ Hz, 1H), 6.24 (s, 2H). ^{13}C NMR (CDCl_3): δ 159.4, 143.3, 142.5, 137.6, 134.6, 132.0, 130.9, 127.0, 124.7, 122.3, 120.0, 118.6. ESMS m/z : 303.5 ($M + 1$) $^+$.

1-(4-Chlorobenzylideneamino)-4-(pyridin-2-yl)-1H-imidazol-2-amine (18). ^1H NMR (CDCl_3): δ 8.73 (s, 1H), 8.48 (d, $J = 4.8$ Hz, 1H), 8.09 (s, 1H), 7.96 (d, $J = 8.4$ Hz, 2H), 7.79–7.15 (m, 2H), 7.56 (d, $J = 8.4$ Hz, 2H), 7.20–7.15 (m, 1H), 6.28 (br, 2H). ^{13}C NMR (CDCl_3): δ 158.4, 156.4, 150.3, 146.5, 139.2, 137.6, 137.0, 132.9, 131.6, 127.0, 126.2, 124.0, 119.8. ESMS m/z : 298.3 ($M + 1$) $^+$.

1-(4-Fluorobenzylideneamino)-4-(pyridin-3-yl)-1H-imidazol-2-amine (19). ^1H NMR (CDCl_3): δ 8.96 (d, $J = 1.8$ Hz, 1H), 8.48 (dd, $J = 4.8, 1.8$ Hz, 1H), 8.20 (s, 1H), 8.05 (dt, $J = 8.1, 1.8$ Hz, 1H), 7.81 (dd, $J = 8.7, 5.4$ Hz, 2H), 7.47 (s, 1H), 7.31 (ddd, $J = 8.1, 4.8, 1.8$ Hz, 1H), 7.18 (t, $J = 8.7$ Hz, 2H), 4.95 (br, 2H). ^{13}C NMR (CDCl_3): δ 166.2, 159.0, 149.5, 148.3, 144.5, 137.0, 133.1, 132.1, 131.8, 129.4, 124.0, 122.0, 117.6. ESMS m/z : 282.3 ($M + 1$) $^+$.

1-(2,3-Dihydronaphthalen-4(1H)-ylideneamino)-4-phenyl-1H-imidazol-2-amine (20). ^1H NMR (CDCl_3): δ 8.31 (d, $J = 7.8$ Hz, 1H), 7.68 (d, $J = 7.2$ Hz, 2H), 7.45–7.38 (m, 2H), 7.32–7.25 (m, 4H), 7.12 (t, $J = 7.2$ Hz, 1H), 5.72 (s, 2H), 2.93 (t, $J = 6.3$ Hz, 2H), 2.85 (t, $J = 6.0$ Hz, 2H), 1.92–1.83 (m, 2H). ^{13}C NMR (CDCl_3): δ 164.4, 140.5, 139.7, 136.4, 133.1, 131.2, 129.3, 129.1, 128.8, 128.6, 128.3, 127.5, 126.2, 122.1, 31.6, 26.5. ESMS m/z : 303.3 ($M + 1$) $^+$, 325.1 ($M + 23$) $^+$.

1-(4-Chlorobenzylideneamino)-4-(thiophen-2-yl)-1H-imidazol-2-amine (21). ^1H NMR (CDCl_3): δ 8.52 (s, 1H), 7.93 (d, $J = 8.4$ Hz, 2H), 7.80 (s, 1H), 7.55 (d, $J = 8.4$ Hz, 2H), 7.35 (d, $J = 4.2$ Hz, 1H), 7.21 (d, $J = 4.2$ Hz, 1H), 7.04 (t, $J = 4.2$ Hz, 1H), 6.31 (br, 2H). ^{13}C NMR (CDCl_3): δ 160.4, 145.3, 138.7, 137.2, 132.9, 131.6, 130.2, 128.9, 128.6, 124.5, 121.3, 118.0. ESMS m/z : 303.4 ($M + 1$) $^+$.

1-(4-Chlorobenzylideneamino)-4,5-diphenyl-1H-imidazol-2-amine (22). ^1H NMR (CDCl_3): δ 7.90 (s, 1H), 7.38 (d, $J = 8.4$ Hz, 2H), 7.49–7.34 (m, 9H), 7.20–7.06 (m, 3H), 6.11 (br, 2H). ^{13}C NMR (CDCl_3): δ 158.4, 137.6, 136.5, 132.4, 132.9, 131.6, 131.5, 129.4, 128.3, 127.0, 126.8, 125.5, 124.5, 122.5, 121.0. ESMS m/z : 373.5 ($M + 1$) $^+$.

1-(4-Chlorobenzylideneamino)-4-(thiazol-2-yl)-1H-imidazol-2-amine (23). ^1H NMR (CDCl_3): δ 8.72 (s, 1H), 8.08 (s, 1H), 7.96 (d, $J = 8.1$ Hz, 2H), 7.79 (d, $J = 3.3$ Hz, 1H), 7.59–7.56 (m, 3H), 6.45 (br, 2H). ^{13}C NMR (CDCl_3): δ 162.2, 157.4, 145.9, 137.6, 135.3, 132.9, 130.4, 127.0, 121.3, 120.3, 116.6. ESMS m/z : 304.5 ($M + 1$) $^+$.

Acknowledgment. This study was supported by Grants BP-090-PP01, BP-090-CF03, and BP-091-CF03 of The National Health Research Institutes, Miaoli, Taiwan.

References

- Uttamchandani, M.; Lu, H. S.; Yao, S. Q. Next generation chemical proteomic tools for rapid enzyme profiling. *Acc. Chem. Res.* **2009**, *42*, 1183–1192.
- Liu, B.; Li, S. J. Technological advances in high-throughput screening. *Am. J. Pharmacogenomics* **2004**, *4*, 263–276.
- Hann, M. M.; Oprea, T. I. Pursuing the leadlikeness concept in pharmaceutical research. *Curr. Opin. Chem. Biol.* **2004**, *8*, 255–263.
- Yang, X.; Chen, E.; Jiang, H.; Muszynski, K.; Harris, R. D.; Giardina, S. L.; Gromeier, M.; Mitra, G.; Soman, G. Evaluation of IRES-mediated, cell-type-specific cytotoxicity of poliovirus using a colorimetric cell proliferation assay. *J. Virol. Methods* **2009**, *155*, 44–54.
- Cory, A. H.; Owen, T. C.; Barltrop, J. A.; Cory, J. G. Use of an aqueous soluble tetrazolium/formazan assay for cell growth assays in culture. *Cancer Commun.* **1991**, *3*, 207–212.
- Thabrew, M. I.; Hughes, R. D.; McFarlane, I. G. Screening of hepatoprotective plant components using a HepG2 cell cytotoxicity assay. *J. Pharm. Pharmacol.* **1997**, *49*, 1132–1135.
- Bleicher, K. H.; Böhm, H.-J.; Müller, K.; Alanine, A. I. A guide to drug discovery: hit and lead generation: beyond high-throughput screening. *Nat. Rev. Drug Discovery* **2003**, *2*, 369–378.
- Bennett, J. L. L.; Baker, H. T. Synthesis of potential anticancer agents. IV. 4-Nitro- and 4-amino-5-imidazole sulfones. *J. Am. Chem. Soc.* **1957**, *79*, 2188–2191.
- Lee, H. H.; Palmer, B. D.; Wilson, W. R.; Denny, W. A. Synthesis and hypoxia-selective cytotoxicity of a 2-nitroimidazole mustard. *Bioorg. Med. Chem. Lett.* **1998**, *8*, 1741–1774.
- Iradyan, M. A.; Iradyan, N. S.; Ovagimyan, A. A.; Stepanyan, G. M.; Arsenyan, F. G.; Garibdzhanyan, B. T. Imidazole derivatives XVIII. Synthesis and antitumor activity of some bis[2-chloroethyl]amino imidazole derivatives. *Pharm. Chem. J.* **1984**, *18*, 462–466.
- Bielawski, K.; Bielawska, A.; Poplawska, B. Synthesis and cytotoxic activity of novel amidine analogues of bis(2-chloroethyl)amine. *Arch. Pharm. Chem. Life Sci.* **2009**, *342*, 484–490.
- LaBarbera, D. V.; Modzelewska, K.; Glazar, A. I.; Gray, P. D.; Kaur, M.; Liu, T.; Grossman, D.; Harper, M. K.; Kuwada, S. K.; Moghal, N.; Ireland, C. M. The marine alkaloid naamidine A promotes caspase-dependent apoptosis in tumor cells. *Anti-Cancer Drugs* **2009**, *20*, 425–436.
- Copp, B. R.; Fairchild, C. R.; Cornell, L.; Casazza, A. M.; Robinson, S.; Ireland, C. M. Naamidine A is an antagonist of the epidermal growth factor receptor and an in vivo active anti-tumor agent. *J. Med. Chem.* **1998**, *41*, 3909–3911.
- Kanthou, C.; Tozer, G. M. Microtubule depolymerizing vascular disrupting agents: novel therapeutic agents for oncology and other pathologies. *Int. J. Exp. Pathol.* **2009**, *90*, 284–294.
- De Rycker, M.; Rigoreau, L.; Dowling, S.; Parker, P. J. A high-content, cell-based screen identifies micropolyin, a new inhibitor of microtubule dynamics. *Chem. Biol. Drug Des.* **2009**, *73*, 599–610.
- Hait, W. N.; Hambley, T. W. Targeted cancer therapeutics. *Cancer Res.* **2009**, *69*, 1263–1267.
- Budman, D. R. Vinorelbine (Navelbine): a third-generation vinca alkaloid. *Cancer Invest.* **1997**, *15*, 475–490.
- Simoni, D.; Romagnoli, R.; Baruchello, R.; Rondanin, R.; Rizzi, M.; Pavani, M. G.; Alloatt, D.; Giannini, G.; Marcellini, M.; Riccioni, T.; Castorina, M.; Guglielmi, M. B.; Bucci, F.; Carminati, P.; Pisano, C. Novel combretastatin analogues endowed with antitumor activity. *J. Med. Chem.* **2006**, *49*, 3033–3044.
- Zhou, J.; Giannakakou, P. Targeting microtubules for cancer chemotherapy. *Curr. Med. Chem.: Anti-Cancer Agents* **2005**, *5*, 10–12.
- Carlson, R. O. New tubulin targeting agents currently in clinical development. *Expert Opin. Invest. Drugs* **2008**, *17*, 707–722.
- Krimer, M. Z.; Makaev, F. Z.; Styngach, E. P.; Koretskii, A. G.; Pogrebnoi, S. I.; Kochug, A. I. Synthesis of substituted 2-amino-1-arylideneaminoimidazoles and 1-arylideneaminoimidazo[1,2-*a*]imidazoles. *Chem. Heterocycl. Compd.* **1996**, *32*, 1035–1039.
- Kolos, N. N.; Orlov, V. D.; Paponov, B. V.; Shishkin, O. V. Synthesis of dihydro derivatives of 2-amino-4,5,7-triarylimidazo[1,5-*b*]pyridazine. *Chem. Heterocycl. Compd.* **1999**, *35*, 1207–1213.
- Quattara, L.; Debaert, M.; Cavier, R. Synthèse et activité antiparasitaire de nouveaux dérivés du nitro-5 imidazol. *Farmaco* **1987**, *42*, 449–456.
- Ivashchenko, A. V.; Lazareva, V. T.; Prudnikova, E. K.; Ivashchenko, S. P.; Romyantsev, V. G. Synthesis of 1, 2-diaminoimidazole guanylhydrazone with α -haloalkyl aryl ketones. *Chem. Heterocycl. Compd.* **1982**, *18*, 185–189.
- Gyoergydeak, Z.; Szabo, G.; Holzer, W. 2-Amino-4-aryl-1-arylideneaminoimidazoles and acylation products: a multinuclear (^1H , ^{13}C , ^{15}N) NMR study. *Monatsh. Chem.* **2004**, *135*, 173–184.

- (26) Mahboobi, S.; Sellmer, A.; Höcher, H.; Eichhorn, E.; Bär, T.; Schmidt, M.; Maier, T.; Stadlwieser, J. F.; Beckers, T. L. [4-(Imidazol-1-yl)thiazol-2-yl]phenylamines. A novel class of highly potent colchicine site binding tubulin inhibitors: synthesis and cytotoxic activity on selected human cancer cell lines. *J. Med. Chem.* **2006**, *49*, 5769–5776.
- (27) Liberatore, A. M.; Coulomb, H.; Pons, D.; Dutruel, O.; Kasprzyk, P. G.; Carlson, M.; Nelson, A. S.; Newman, S. P.; Stengel, C.; Auvray, P.; Hesry, V.; Foll, B.; Narboux, N.; Morlais, D.; Le Moing, M.; Bernetiere, S.; Dellile, R.; Camara, J.; Ferrandis, E.; Bigg, D. C.; Prévost, G. P. IRC-083927 is a new tubulin binder that inhibits growth of human tumor cells resistant to standard tubulin-binding agents. *Mol. Cancer Ther.* **2008**, *7*, 2426–2434.
- (28) Goodwin, C. J.; Holt, S. J.; Downes, S.; Marshall, N. J. Microculture tetrazolium assays: a comparison between two new tetrazolium salts, XTT and MTS. *J. Immunol. Methods* **1995**, *179*, 95–103.
- (29) Chuu, J.-J.; Liu, J. M.; Tsou, M. H.; Huang, C.-L.; Chen, C.-P.; Wang, H.-S.; Chen, C.-T. Effects of paclitaxel and doxorubicin in histocultures of hepatocellular carcinomas. *J. Biomed. Sci.* **2007**, *14*, 233–244.
- (30) Li, W. T.; Hwang, D. R.; Chen, C. P.; Shen, C. W.; Huang, C. L.; Chen, T. W.; Lin, C. H.; Chang, Y. L.; Chang, Y. Y.; Lo, Y. K.; Tseng, H. Y.; Lin, C. C.; Song, J. S.; Chen, H. C.; Chen, S. J.; Wu, S. H.; Chen, C. T. Synthesis and biological evaluation of N-heterocyclic indolyl glyoxylamides as p.o. active anticancer agents. *J. Med. Chem.* **2003**, *46*, 1706–1715.
- (31) Zuse, A.; Schmidt, P.; Baasner, S.; Böhm, K. J.; Müller, K.; Gerlach, M.; Günther, E. G.; Unger, E.; Prinz, H. Sulfonate derivatives of naphtho[2,3-*b*]thiophen-4(9*H*)-one and 9(10*H*)-anthracenone as highly active antimicrotubule agents. Synthesis, antiproliferative activity, and inhibition of tubulin polymerization. *J. Med. Chem.* **2007**, *50*, 6059–6066.
- (32) Prinz, H.; Ishii, Y.; Hirano, T.; Stoiber, T.; Camacho Gomez, J. A.; Schmidt, P.; Düsselmann, H.; Burger, A. M.; Prehn, J. H.; Günther, E. G.; Unger, E.; Umezawa, K. Novel benzylidene-9(10*H*)-anthracenones as highly active antimicrotubule agents. Synthesis, antiproliferative activity, and inhibition of tubulin polymerization. *J. Med. Chem.* **2003**, *46*, 3382–3394.
- (33) Kuo, C. C.; Hsieh, H. P.; Pan, W. Y.; Chen, C. P.; Liou, J. P.; Lee, S. J.; Chang, Y. L.; Chen, L. T.; Chen, C. T.; Chang, J. Y. BPR0L075, a novel synthetic indole compound with antimitotic activity in human cancer cells, exerts effective antitumoral activity in vivo. *Cancer Res.* **2004**, *64*, 4621–4628.
- (34) Singer, W. D.; Hersh, R. T.; Himes, R. H. Effect of solution variables on the binding of vinblastine to tubulin. *Biochem. Pharmacol.* **1988**, *37*, 2691–2696.